Supplementary material for "Downscaling of air pollutants in Europe using uEMEP_v6"

Qing Mu[1], Bruce Rolstad Denby[1], Eivind Grøtting Wærsted[1], and Hilde Fagerli[1]

[1]The Norwegian Meteorological Institute, Henrik Mohns Plass 1, 0313, Oslo, Norway

Correspondence: Qing Mu (qingm@met.no)

S1 NO_2 chemistry schemes

Included in uEMEP are a number of simplified NO_2 chemistry schemes, used to derive downscaled NO_2 concentrations from NO_X and O_3 concentrations. The results presented in this paper have used the weighted travel time parcel method, as applied and described in Denby et al. (2020), together with the frequency distribution correction scheme (Section 2.4). In addition to this parameterisation two other chemistry based formulas are available. The first being the photo-stationary formulation, also described in Denby et al. (2020), and the second a stationary formulation that allows for deviation from the photo-stationary state that may be caused by emissions, advection gradients or additional chemistry (Maiheu et al., 2017). Two empirical formulations are also included that are based on a fit to measurement data. The first, the Romberg scheme (Romberg et al., 1996), is already described in Denby et al. (2020) and directly converts NO_X to NO_2 concentrations. The parameters for this equation have been updated by fitting to all available Airbase data for the year 2017. The second empirical scheme, the SRM scheme (Wesseling and van Velze, 2014), includes background O_3 and NO_2 combined with local NO_X as input parameters. The advantage of the two empirical fits is that they should convert NO_X to NO_2 in a manner that is consistent with the observations, and as such can be applied to annual mean concentrations without correcting for non-linear chemistry. The first method is already described in (Denby et al., 2020), the remaining methods are presented in the following sections.

S1.1 Stationary scheme based on EMEP equilibrium

The solution to the photo-stationary equilibrium of NO_2 that only considers the NO_X titration of O_3 (reaction rate k_1) and the photo-disassociation of NO_2 (photo-disassociation rate J) is already presented in Section 2.4. This steady state solution implies

$$\frac{k_1[NO][O_3]}{J[NO_2]} = 1 \tag{S1}$$

For the case where there is equilibrium but other terms such as emissions, deposition or additional chemistry are involved then we can define a constant λ such that

$$\frac{k_1[NO][O_3]}{J[NO_2]} = \lambda \tag{S2}$$

For $\lambda < 1$ this implies a sink of NO_2 and for $\lambda > 1$ a source. The steady state solution can then be written, as in Eq. (1), as

$$[NO_2] = \frac{1}{2}\left(([NO_X] + [O_X] + \lambda J/k_1) - \sqrt{([NO_X] + [O_X] + \lambda J/k_1)^2 - 4[NO_X][O_X]}\right) \tag{S3}$$

By simply extracting the parameters listed in Eq. (S1) from the EMEP model we can determine λ and by using Eq. (S3) we can calculate the downscaled NO_2 concentrations. At the station sites used in this study we find on average $\lambda = 0.95$ with a standard deviation of 0.35. Around 60% of the sites have $\lambda < 1$. This means there is significant divergence from the photo-stationary assumption in the EMEP annual mean calculations. λ is also strongly correlated with NO_2, increasing with increasing NO_2, indicating that emissions are perhaps the dominating factor leading to non photo-stationary equilibrium. It should be noted that the term $[NO_X] + [O_X]$ in Eq. (S3) is usually significantly larger than J/k_1 so even with a significant deviation of λ from unity then the NO_2 concentrations will not be largely affected.

This parameterisation is particularly useful if NO_2 concentrations from EMEP are to be recalculated, for example when using the local fraction to assess the impact on concentrations with changes in emissions in a post-processing step. It is not necessarily the case that the conditions leading to a deviation of λ from unity are equally applicable for the downscaling chemistry.

S1.2 Updated Romberg scheme

The Romberg scheme (Romberg et al., 1996) is the simplest method for converting NO_X to NO_2. It is based on an empirical fit to the formula

$$[NO_2] = a\frac{[NO_X]}{[NO_X] + b} + c[NO_X] \tag{S4}$$

The parameters a, b ($\mu g/m^3$) and c are derived by fitting to observed annual mean concentrations. The term c should in some way reflect the ratio of NO_2/NO_X emissions, i.e. the asymptotic limit for large NO_X. Values for these parameters were given in Denby et al. (2020), based on a fit to Norwegian measurement data. For the European application a new fit is made to

annual mean concentrations from all available European observations for 2017. This is shown in Fig. S1. The fitted parameters are: $a = 41.1$, $b = 56.4\ \mu g/m^3$ and $c = 0.162$. The root mean square error of this fit is 2.9 $\mu g/m^3$, or a normalised error of around 14%.

When implemented in uEMEP a small adjustment is made to Eq. (S4). It is desirable that background NO_2 levels provided by EMEP are not altered by this calculation. Background NO_2 and O_3 concentrations are calculated in uEMEP after the removal of the local fraction contribution from NO_X. In Denby et al. (2020) this is referred to as the non-local contribution. To achieve this we rewrite Eq. (S4) as follows

$$[NO_2] = a\frac{[NO_X]}{[NO_X]+b} + c[NO_X] + \Delta[NO_2]_{bg} \tag{S5}$$

where $\Delta[NO_2]_{bg}$ is the difference between the EMEP calculated NO_2 non-local contribution and the Romberg calculation of the non-local contribution given by

$$\Delta[NO_2]_{bg} = [NO_2]_{nonlocal} - a\frac{[NO_X]_{nonlocal}}{[NO_X]_{nonlocal}+b} + c[NO_X]_{nonlocal} \tag{S6}$$

This ensures that the calculated NO_2 concentrations are unchanged when the local contribution to NO_X is negligible.

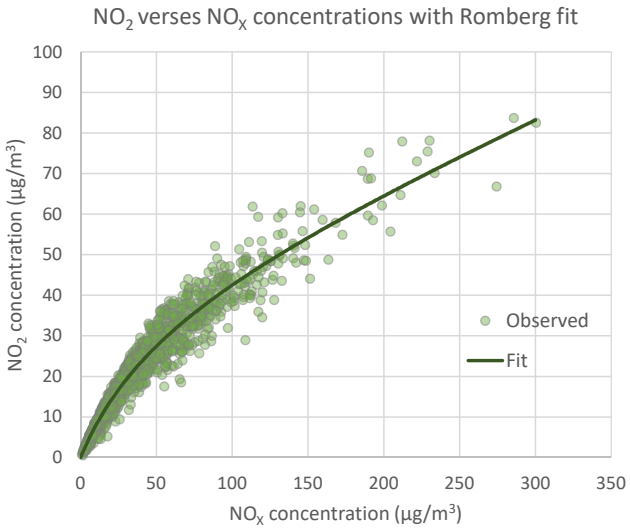

Figure S1. Annual mean NO_2 verses NO_X concentrations for 2017 showing 1774 available Airbase stations. The fit using the Romberg equation is also shown, using the parameters provided in the text.

S1.3 SRM scheme

The SRM scheme for NO_2 calculation is implemented in The Netherlands as part of the Standard Calculation Method for air quality (Wesseling and van Velze, 2014). This scheme requires information on background levels of O_3 and NO_2. Whilst this information is directly available from the model calculations this is more difficult to extract from measurement data. For this reason no fitting or changes to the parameters given in Wesseling and van Velze (2014) have been made. The equation is slightly re-written to be comparable with the Romberg scheme and the uEMEP formulation as:

$$[NO_2] = [NO_2]_{bg} + [O_3]_{nonlocal}\frac{[NO_X]_{local}}{[NO_X]_{local} + b_{srm}} + c_{srm}[NO_X]_{local} \quad \text{(S7)}$$

where

$$b_{srm} = \frac{100}{1 - c_{srm}} \text{ and } c_{srm} = 0.15$$

The value for c_{srm} applied here is the traffic exhaust NO_2/NO_X emission ratio used in uEMEP, and the value for b_{srm} $(\mu g/m^3)$ comes directly from Wesseling and van Velze (2014). The parameters c_{srm} and b_{srm} are refered to as F and K respectively in Wesseling and van Velze (2014).

This equation clearly resembles the Romberg scheme, Eq. (S4), with the exception that a background NO_2 and a local NO_X are used. Here the background ozone would then be equivalent to the parameter $a_{srm} = [O_3]_{nonlocal}$.

S1.4 Additional information on the frequency distribution correction scheme

A frequency distribution correction scheme for annual mean calculations of NO_2 is described in Section 2.4. This is implemented to deal with the non-linear nature of the NO_2 chemistry when calculating annual means. Here we present some of the background information used to derive this scheme.

An example of the NO_X, O_X and J frequency distributions is shown in Fig. S2. Here we see the log-normal distribution of the concentrations and the quite different distribution of the photo-dissociation rate J. J has a frequency of close to 0.5 at $J = 0$, since this, over the course of a year, is the amount of time the sun is below the horizon. The example shown here is taken from a low latitude European urban background station, with moderate NO_X and high O_3.

An assessment of measurement and model data for 2018 was carried out for Norwegian stations in order to derive the standard deviations of the NO_X and O_X concentrations. This assessment was limited to available data and a more substantial assessment could be carried out on a larger set of data. Focus is on the modelled distributions since this is what needs to be reproduced in order to correct the annual mean calculation. Firstly the concentration distributions were tested for a log-normal distribution. An example for both NO_X and O_X, both modelled and observed is shown for the urban background station Klosterhaugen in Bergen, Norway, in Fig. S3 and Fig. S4. This is one of the few stations measuring both NO_X and O_3 in

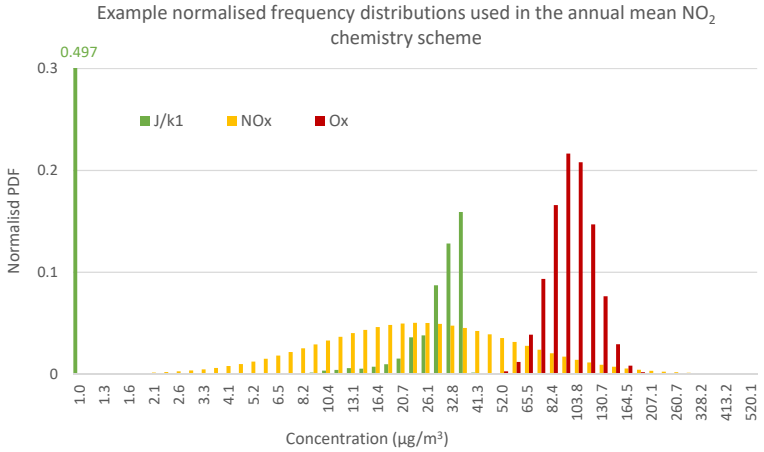

Figure S2. Example of the frequency distribution for NO_X, O_X and J concentrations used in the model. This is taken from the calculation of an actual site in Southern Europe. X axis is logarithmic.

Norway. Further assessment of the log-normal distribution was carried out for all modelled data at the 72 sites modelled in Norway for that year. This assessment showed that the concentrations were very close to log-normally distributed at all sites.

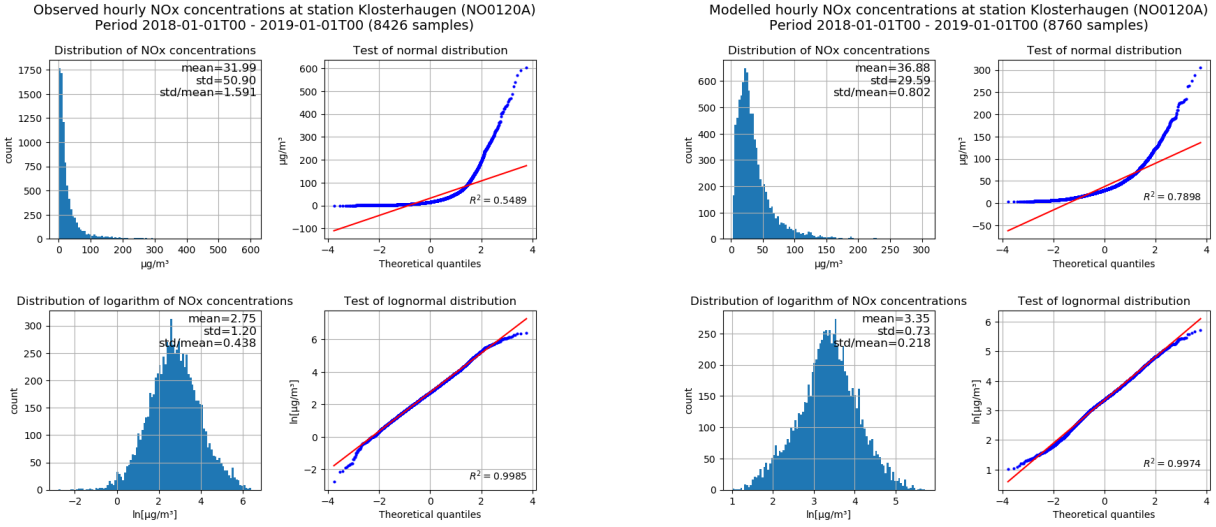

Figure S3. Measured and modelled NO_X distributions for year 2018 at the station Klosterhaugen, Bergen, shown on both a linear and a logarithmic scale.

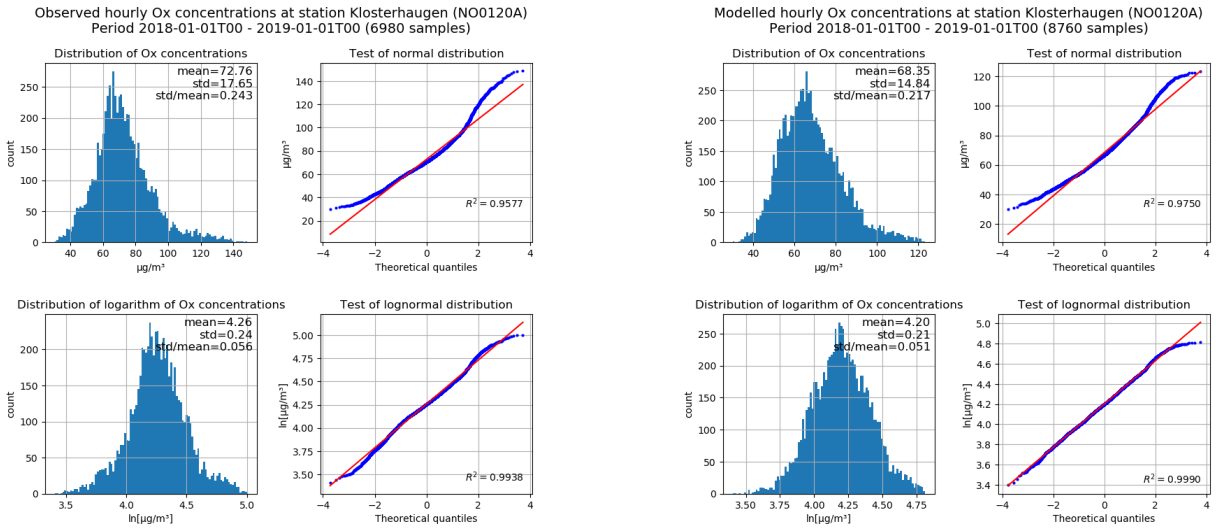

Figure S4. Measured and modelled O_X distributions for year 2018 at the station Klosterhaugen, Bergen, shown on both a linear and a logarithmic scale.

The standard deviations were then derived and compared to mean values. The results for both NO_X and O_X at modelled stations are shown in Fig. S5. For NO_X the observed values are also included since these are more readily available. The relationship for NO_X is very robust and will reflect the temporal variation of the NO_X sources, mostly traffic, and of the meteorology. It is worth noting that the normalised standard deviation of the traffic time profile applied in the Norwegian calculations is 0.71. Additional variability will be added due to meteorology. For O_X the standard deviation is less dependent on the mean concentration. Even so, the normalised standard deviation of O_X is significantly smaller than that of NO_X.

Finally the correlation between NO_X and O_X was addressed since the frequency distribution correction assumes these two concentrations are not correlated. This assessment showed both negative and positive correlations at the modelling sites. Sites with high NO_X concentrations showed positive correlation and background sites showed mostly negative correlation. Since NO_2 is part of both NO_X and O_X then this positive correlation is not surprising. Values for the correlation (r) ranged from -0.4 to +0.6. This result shows there is correlation between NO_X and O_X but this would be difficult to take account of in the frequency distribution correction currently implemented in the model.

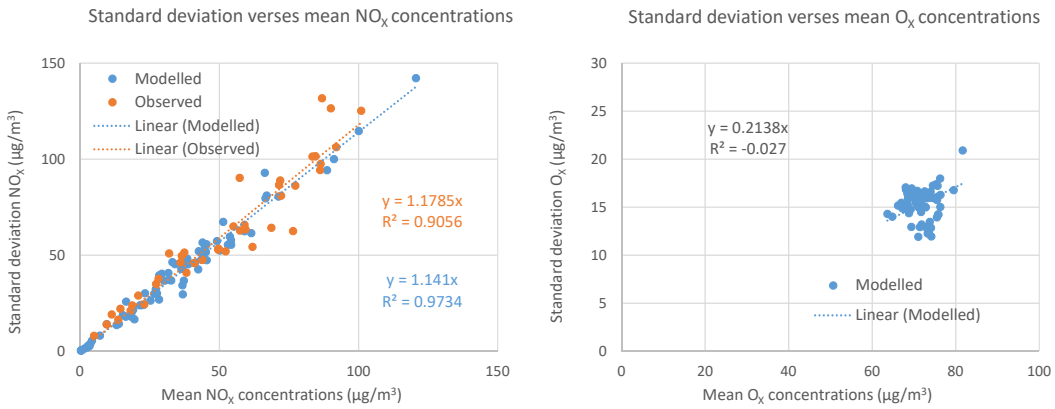

Figure S5. Scatter plot of hourly standard deviation verses annual mean NO_X and O_X for 2018 for all the 72 modelled sites. Also include are measurement data from 41 of the sites that measured NO_X with data coverage >75%. The regression slope, intercept set to 0, and the correlation are also shown in the plots.

S2 Scatter plots per country

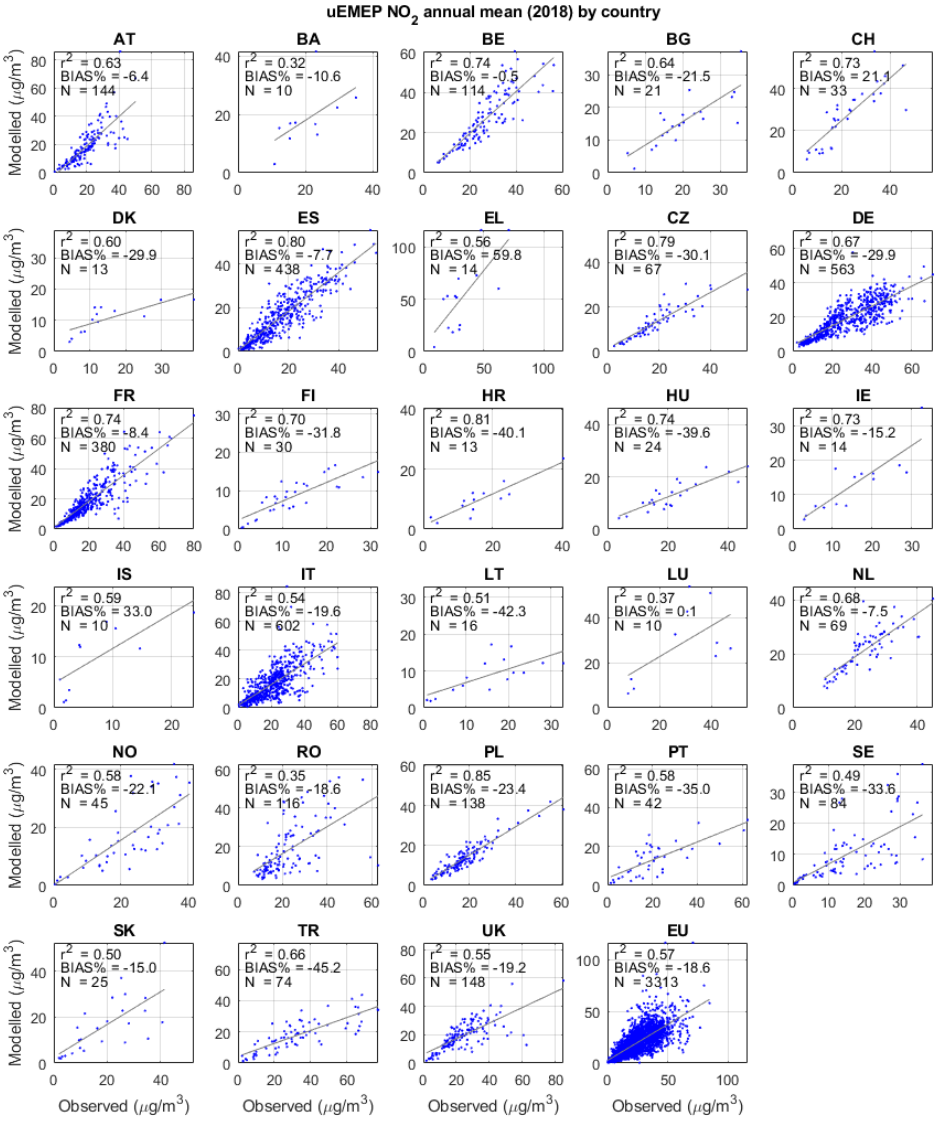

Figure S6. Scatter plots of annual mean NO_2 concentrations per country for 2018 calculated with uEMEP. Only countries with 10 or more stations are shown individually but all stations are included in the final EU plot.

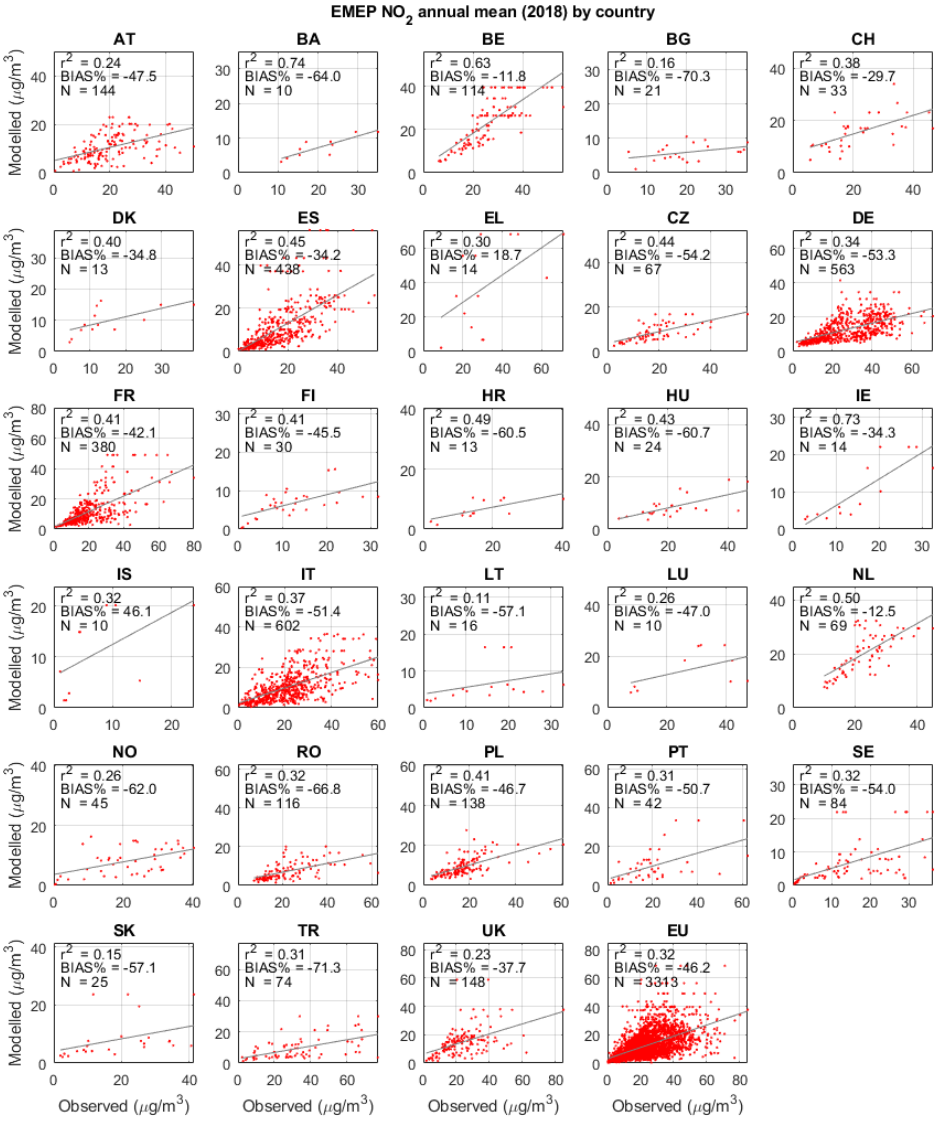

Figure S7. Scatter plots of annual mean NO_2 concentrations per country for 2018 calculated with EMEP. Only countries with 10 or more stations are shown individually but all stations are included in the final EU plot.

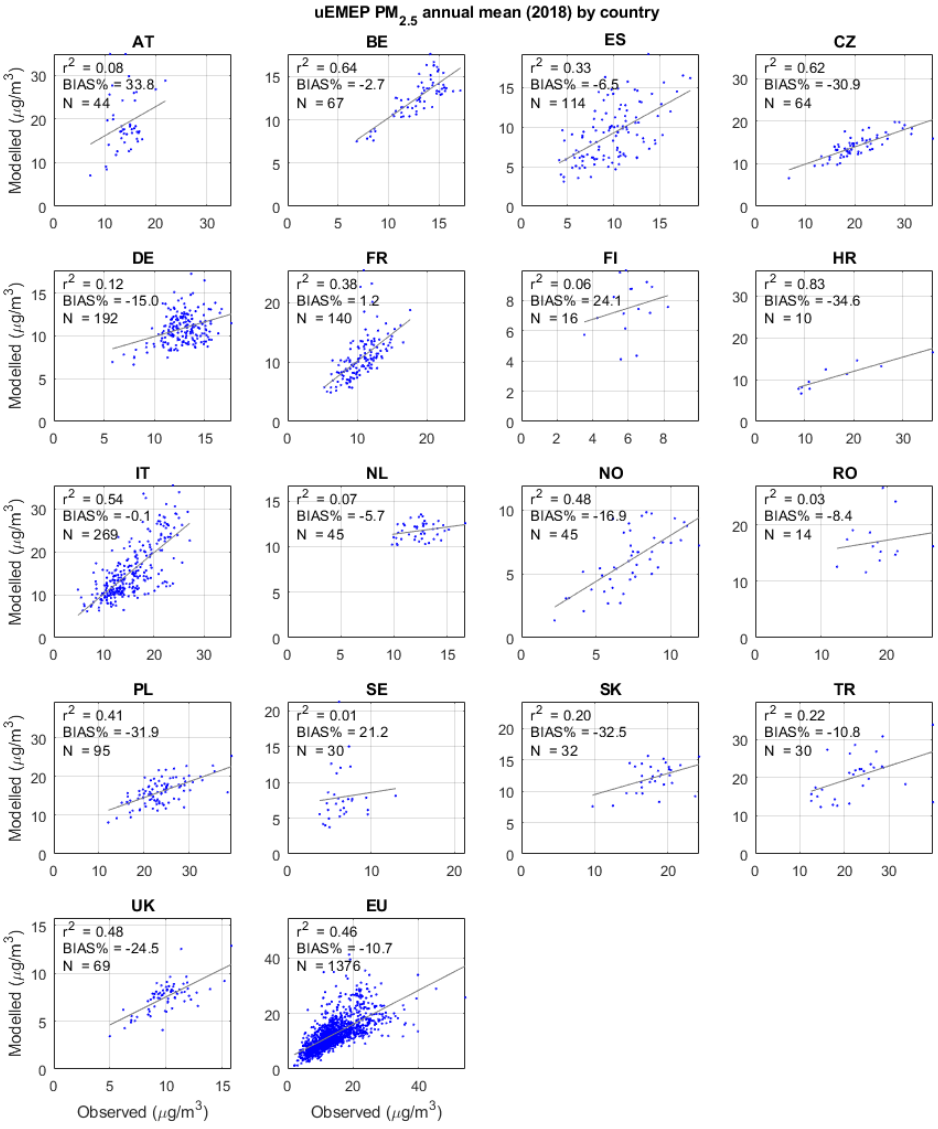

Figure S8. Scatter plots of annual mean $PM_{2.5}$ concentrations per country for 2018 calculated with uEMEP. Only countries with 10 or more stations are shown individually but all stations are included in the final EU plot.

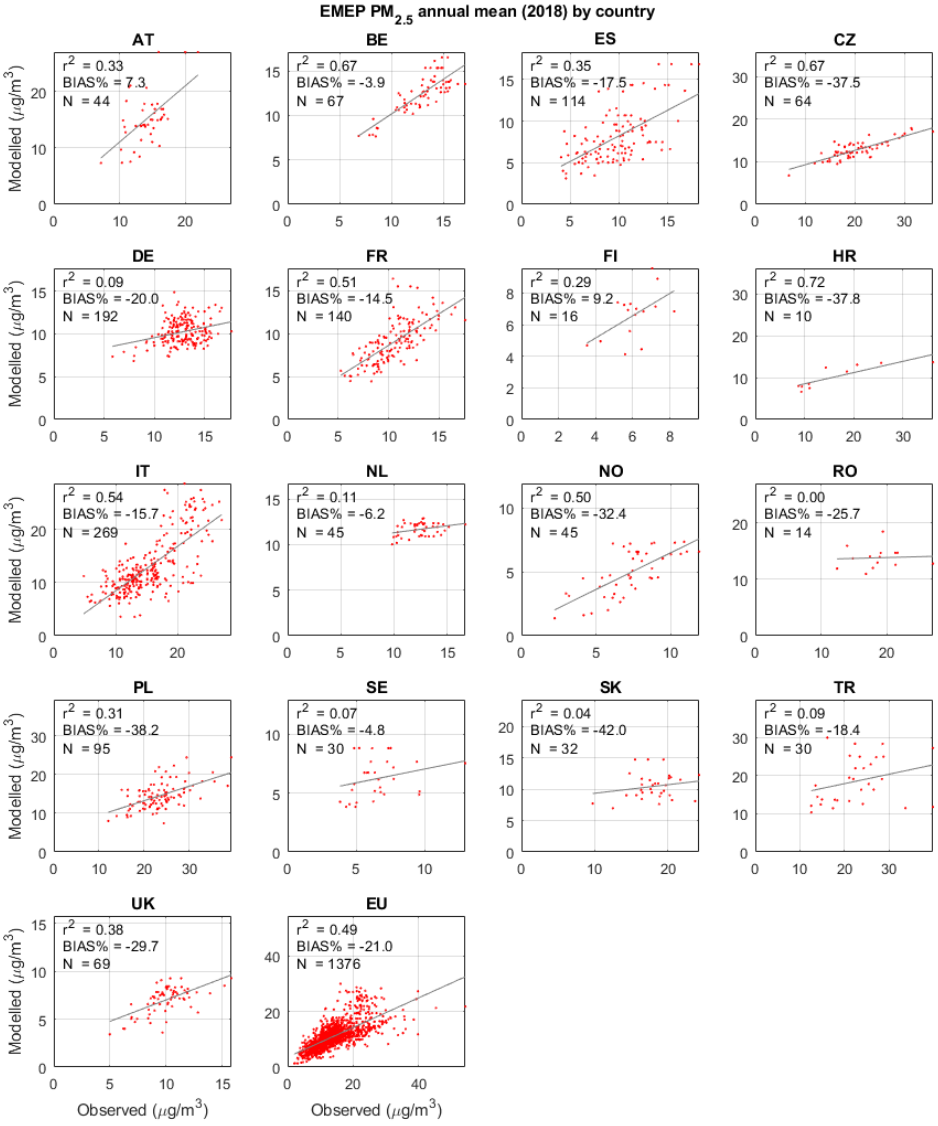

Figure S9. Scatter plots of annual mean $PM_{2.5}$ concentrations per country for 2018 calculated with EMEP. Only countries with 10 or more stations are shown individually but all stations are included in the final EU plot.

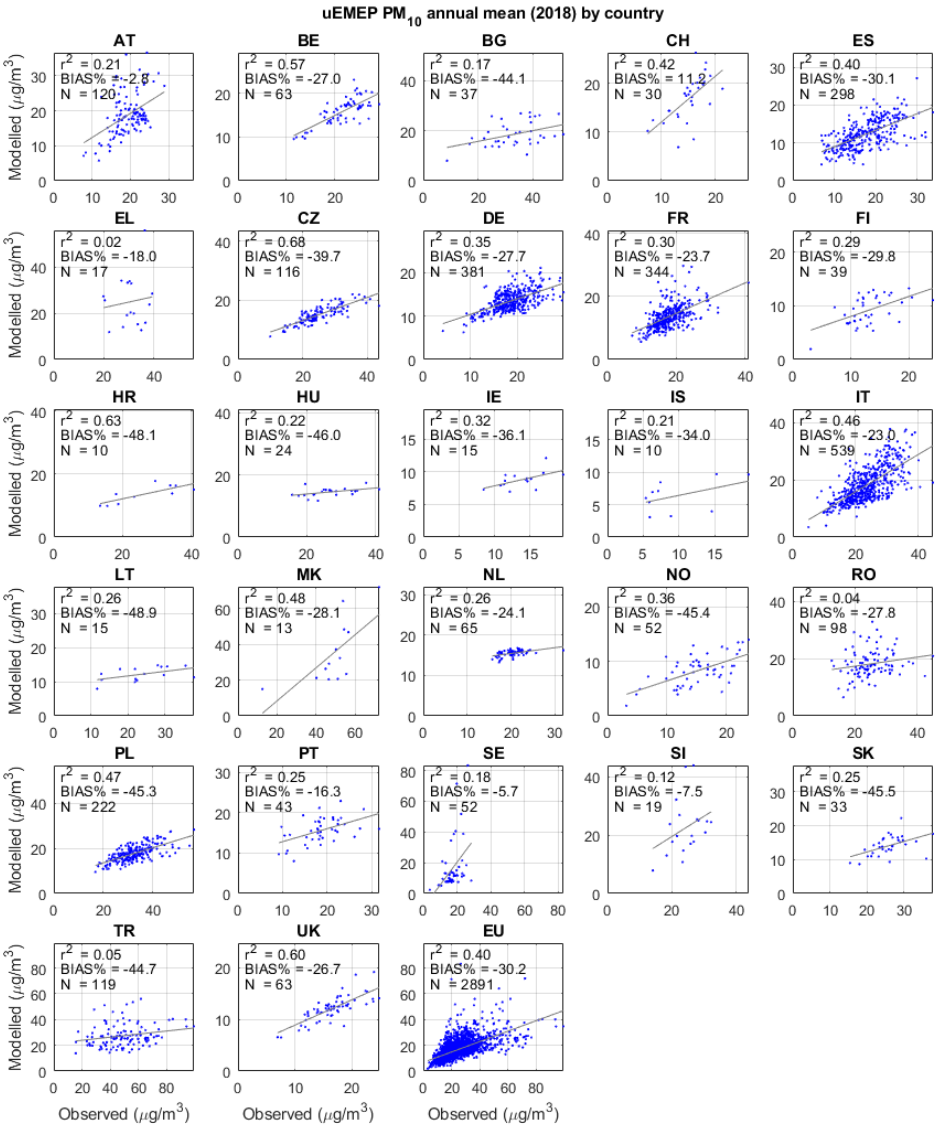

Figure S10. Scatter plots of annual mean PM_{10} concentrations per country for 2018 calculated with uEMEP. Only countries with 10 or more stations are shown individually but all stations are included in the final EU plot.

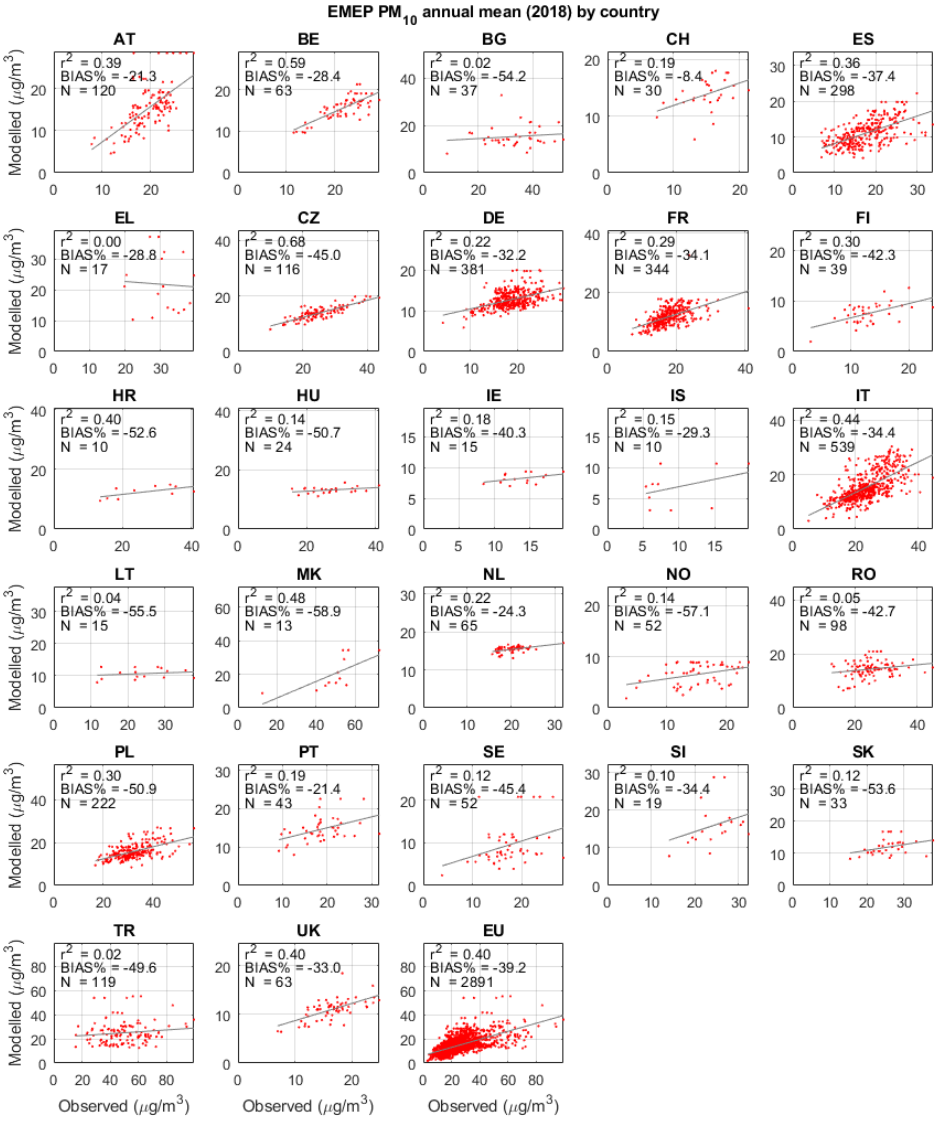

Figure S11. Scatter plots of annual mean PM_{10} concentrations per country for 2018 calculated with EMEP. Only countries with 10 or more stations are shown individually but all stations are included in the final EU plot.

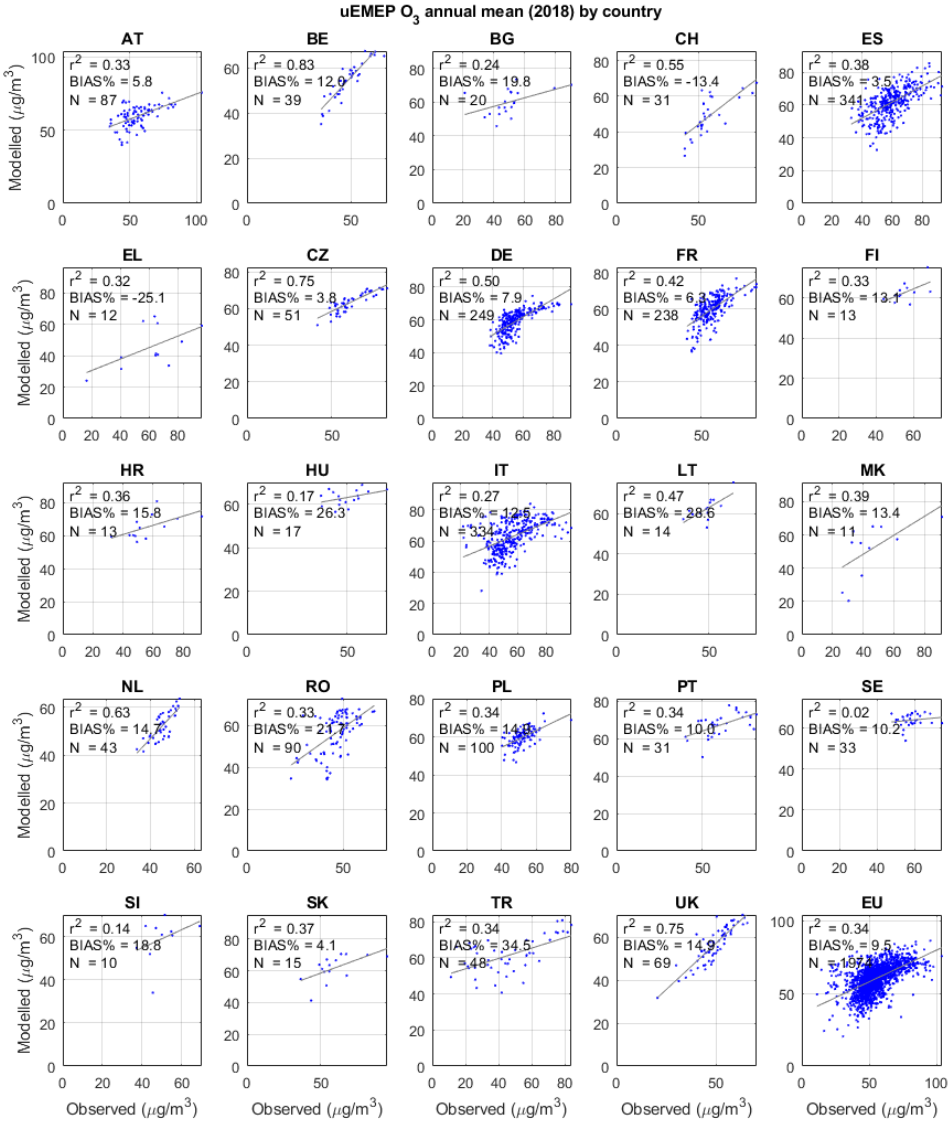

Figure S12. Scatter plots of annual mean O_3 concentrations per country for 2018 calculated with uEMEP. Only countries with 10 or more stations are shown individually but all stations are included in the final EU plot.

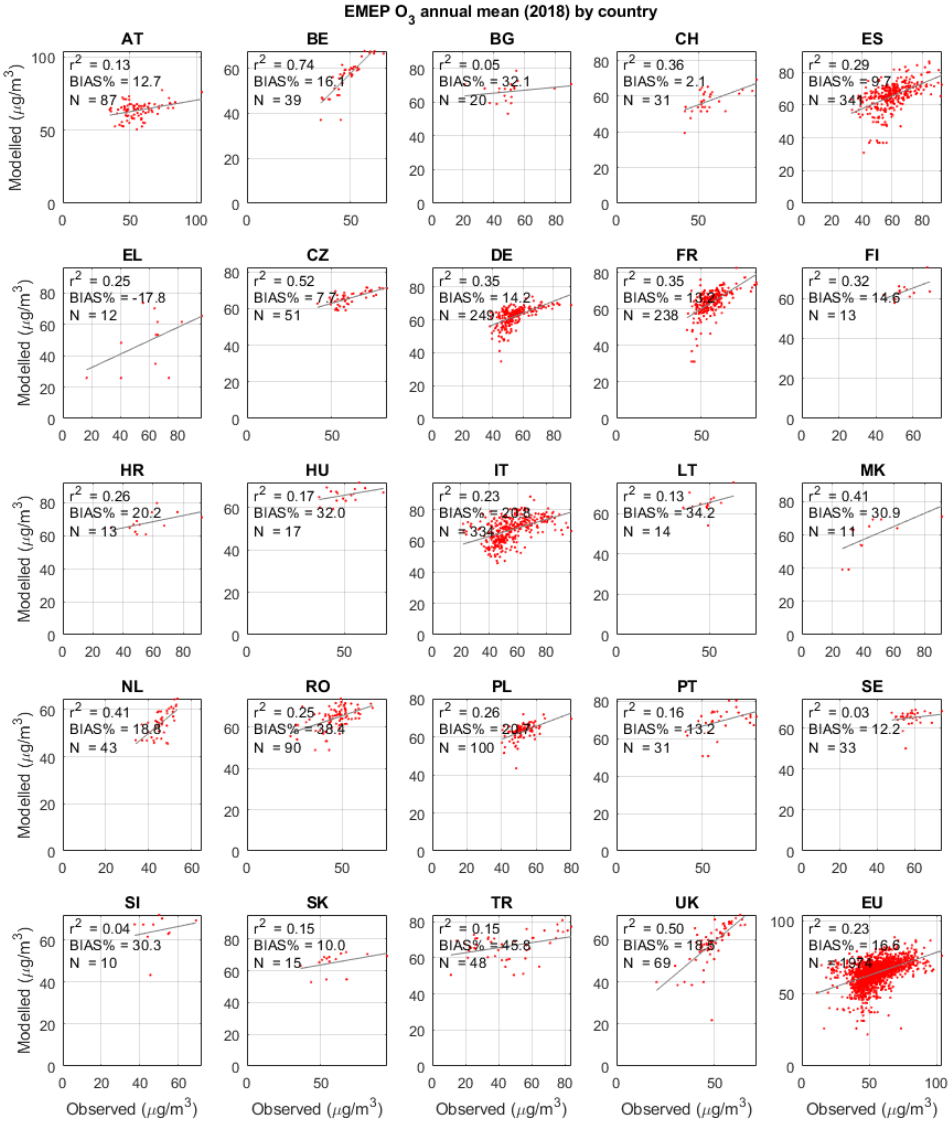

Figure S13. Scatter plots of annual mean O_3 concentrations per country for 2018 calculated with EMEP. Only countries with 10 or more stations are shown individually but all stations are included in the final EU plot.

References

Denby, B. R., Gauss, M., Wind, P., Mu, Q., Grøtting Wærsted, E., Fagerli, H., Valdebenito, A., and Klein, H.: Description of the uEMEP_v5 downscaling approach for the EMEP MSC-W chemistry transport model, Geosci. Model Dev., 13, 6303–6323, https://doi.org/10.5194/gmd-13-6303-2020, 2020.

Maiheu, B., Williams, M. L., Walton, H. A., Janssen, S., Blyth, L., Velderman, N., Lefebvre, W., Vanhulzel, M., and Beevers, S. D.: Improved Methodologies for NO2 Exposure Assessment in the EU, Vito Report no. 2017/RMA/R/1250, Tech. Rep. https://ec.europa.eu/environment/air/publications/models.htm, 2017.

Romberg, E., Bosinger, R., Lohmeyer, A., Ruhnke, R., and Röth, E.: NO-NO2-Umwandlung für die Anwendung bei Immissionsprognosen für Kfz-Abgase, Gefahrstoffe, Reinhaltung der Luft, 56, 215–218, 1996.

Wesseling, J. and van Velze, K.: Technische beschrijving van standaardrekenmethode 2 (SRM-2) voor luchtkwaliteitsberekeningen, Tech. Rep. https://core.ac.uk/download/pdf/58774365.pdf, 2014.